Journal of the Australian Ceramic Society (2020) 56:203–215
https://doi.org/10.1007/s41779-019-00352-4

RESEARCH

Modification of surface charge characteristics for unsupported nanostructured titania–zirconia UF/NF membrane top layers with calcination temperature

İlker Erdem[1] · Muhsin Çiftçioğlu[2]

Received: 10 November 2017 / Revised: 15 August 2018 / Accepted: 10 April 2019 / Published online: 18 April 2019

Abstract

Ceramic membranes are more advantageous alternatives especially for harsh working conditions when compared with the polymeric membranes. The porous multilayer structure of the ceramic membranes (composed of support, intermediate, and top layers) can be prepared via different oxides. Titania and zirconia, having superior properties, are mainly preferred for the top layer formation. The separation properties of the membrane are both dependent on pore morphology and surface charge of the oxide(s) forming the top layer. The effect of surface charge in separation may be very significant in case of filtration of charged species with relatively lower mass as in the ultrafiltration (UF) and nanofiltration (NF). In this study, unsupported membrane top layers were prepared with varying titania/zirconia ratios by sol-gel technique. Their surface charges at different pH conditions after calcination at varying temperatures (400°, 500°, and 600 °C) were determined. The surface charge of the pure titania (full Ti) top layer was decreasing with the increasing calcination temperature. The highest magnitudes of zeta potential for both acidic and basic conditions were measured via Zr rich top layer (TiZr2575) at calcination temperatures ≥ 500 °C, which was composed of anatase, rutile (titania), and tetragonal (zirconia) phases after calcination. The tailor-made top layer can be prepared with modifications during membrane preparation.

Keywords Titania · Zirconia · Membrane · Calcination · Surface charge

Introduction

Ceramic membranes possess some superior properties when compared with their polymeric antecedents. Thermal, chemical, physical, and microbiological durability are some of these, which enable the utilization of ceramic membranes for various applications especially in harsh conditions [1–3]. The porous ceramic membranes can be utilized for filtration with possible purposes of separation, clarification, concentration, etc. Especially for concentration/separation processes to handle heat-sensitive compounds (like proteins, amino acids, etc.) in the liquid media, the pressure-driven filtration applications are more advantageous when compared with concentration processes with heat application (e.g., evaporation). The pressure-driven liquid filtration processes are grouped with respect to the size of the material to be separated in the liquid media. The microfiltration (MF) can be utilized for separation of microorganisms (mainly bacteria), while ultrafiltration would be necessary for separation/concentration of smaller organic materials like proteins. The separation/concentration of even smaller organic materials like pesticides or amino acids may be performed via nanofiltration (NF). The removal of salts can be done through reverse osmosis (RO). The necessary pore size of the porous membrane in pressure-driven liquid filtration applications is expected to decrease with decreasing size of the material to be kept/filtered by the porous membrane. The porous membranes with varying pore sizes necessary for different applications (e.g., MF, UF, NF) should be prepared separately with well-controlled pore sizes and/or separation characteristics.

✉ İlker Erdem
ilker.erdem@agu.edu.tr

[1] Faculty of Engineering, Material Science and Nanotechnology Engineering Department, Abdullah Gül University, Sümer Campus, Barbaros Mh., Kocasinan, Kayseri, Turkey

[2] Chemical Engineering Department, İzmir Institute of Technology, Urla, İzmir, Turkey

In the preparation of porous ceramic membranes alumina, silica, zirconia, and titania are widely used [1]. Commercial porous ceramic membranes are generally multilayered in structure, mainly composed of an alumina support, an intermediate layer, and a top layer [4]. Considering the multilayered structure of the porous ceramic membranes shown in Fig. 1, the support is mainly responsible for mechanical durability of the membrane. It is composed of relatively bigger particulates partially sintered to have a porous structure. The intermediate layer (interlayer) is composed of relatively smaller particles than the ones in the support layer, resulting in a porous layer with smaller pores than of the support layer. Above all, there is the top layer (membrane layer) composed of the tiniest particles and having the finest pores among the three layers mentioned [4].

Titania or zirconia is especially preferred for the top layer. Silica is also widely used for top layer formation due to its remarkable separation/permeation capabilities, but its low durability at harsh conditions (i.e., low thermal, chemical stability) force researchers to develop new materials for top layer formation [5]. There are also some commercial ceramic membranes composed of sole titania (e.g., TAMI Industries—Filtanium series).

Titania and zirconia are distinguishing among other ceramic materials with their durability at high acidic and basic conditions (pH 1–14) [6]. They are used as additives to increase the stability properties of other oxides [2]. Therefore, titania and zirconia are two major oxides especially for applications in media with harsh conditions. They may be used solely [7] or in mixed form. When used in mixed form, the crystallization temperature was reported to increase [2, 6]. This increase in the crystallization temperature was reported to be important to preserve nanoporosity at higher calcination temperatures [6]. The preservation of the microporous structure for the necessary calcination temperature range [7] may be beneficial for both membrane applications and other applications like catalytic support preparation. The SEM micrographs of the unsupported zirconia membranes calcined at different temperatures show the presence of a network of nanoparticles with sizes around 15–40 nm for all calcination (Fig. 2). Similar preservation of the zirconia microstructure after calcinations in the 300–600 °C range for 2 h were also reported [8]. The microstructure may even be preserved at relatively higher calcination temperatures when mixed oxides are being calcined (e.g., zirconia–titania).

The main factor affecting the total specific surface area was reported to be the calcination temperature for zirconia, in contrast with silica, which was reported as the pH of silica sol during sol-gel procedure [9].

The porosity of the top layer mainly determines the rejection capability of the multilayer ceramic membrane (i.e., size exclusion). The surface characteristics (e.g., zeta potential) of the membrane top layer become more effective on the rejection capability of the ceramic membrane with decreasing pore sizes (i.e., Donnan exclusion). Ceramic membranes gain positive or negative surface charge with respect to their own characteristics (i.e., amphoteric behavior) and the pH and ion concentration of the liquid medium to be filtered. The interaction of the amphoteric membrane surface and the ionic groups in the liquid medium affects the permeability flux values as well as retention values [10, 11]. Shang et al. [11] reported the phosphate rejection of the titania ceramic membranes with 3 kDa MWCO (molecular weight cutoff) (i.e., with larger pores) was greater than the 1 kDa MWCO membrane since the former has a greater negative surface charge. (MWCO refers to the smallest size of the material to be separated with a capability of 90%).

Ceramic membranes with fine microporous top layers used for ultrafiltration (UF) and nanofiltration (NF) applications are currently commercially available. The ceramic NF membranes are relatively new in the market. The optimization of the surface characteristics of such ceramic membranes with fine microporous top layers considering both size exclusion and Donnan exclusion mechanisms is important for preparation/selection of the membrane for particular applications.

The ceramic membranes with a tailor-made top layer (a top layer with which possesses the desired characteristics for a particular filtration application) will increase the efficiency

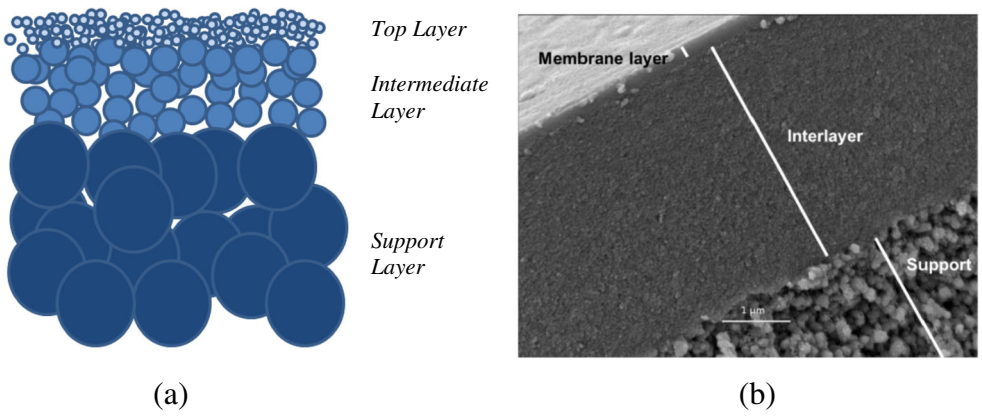

Fig. 1 The possible layers of a porous ceramic membrane with asymmetrical structure, **a** schematic and **b** SEM (scanning electron microscope) micrograph of the cross-section showing these layers [4]

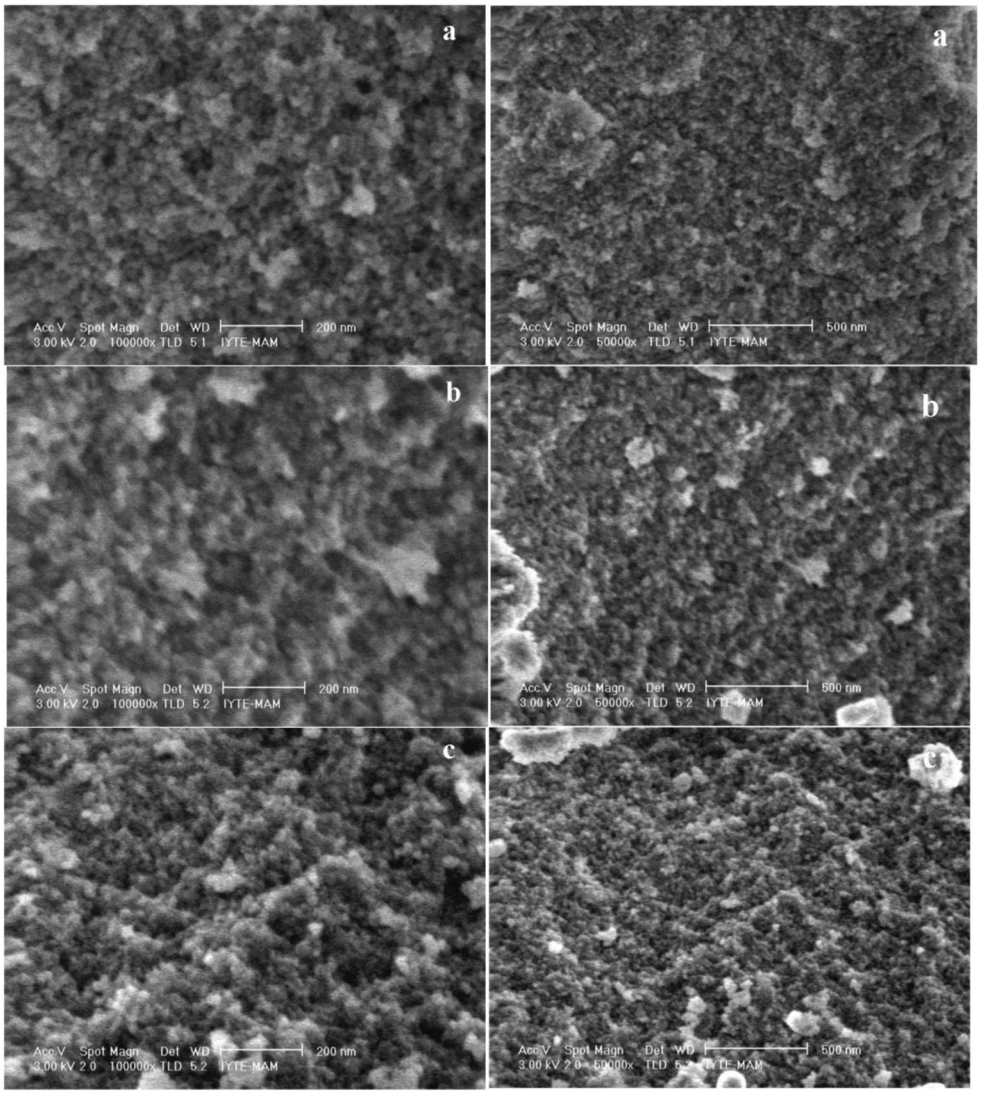

Fig. 2 The SEM micrographs of the zirconia nanoparticles calcined at **a** 400°, **b** 450°, and **c** 500 °C at two different magnifications. Through the lens detector (TLD) was used, applied voltage was 3 kV for the SEM analysis. The magnification for micrographs on the left is × 100,000, while it is × 50,000 for the micrographs on the right. The bar for the micrographs on the left is showing 200 nm in length, and 500 nm length for the micrographs on the right [7]

of the filtration in both retention and permeate flux concerns. In this study, unsupported membranes (top layers) with varying titania/zirconia content were prepared and investigated for their physicochemical characteristics (i.e., crystallographic morphology, surface charge) changing with varying calcination temperatures.

Experimental

Polymeric titania/zirconia sols were prepared by starting with alkoxide(s) (titanium propoxide (98%) and/or zirconium propoxide (70% in propanol)), propanol, and nitric acid, with molar ratios of 1/15−20/1, respectively. The molar ratios of Ti and Zr were arranged to be 0–100% and coded TiZr (mol percentage of Ti) (mol percentage of Zr) (e.g., TiZr 7525). The sols composed of pure Ti or Zr were coded with "full Ti" and "full Zr", respectively. The sols were prepared by addition of nitric acid and a fraction of necessary propanol on the propanol-alkoxide mixture dropwise as explained in former works [7, 12].

The particle size distributions of the sols were determined by using a laser light–scattering instrument (Zetasizer 3000HSA, Malvern, Co., UK). Unsupported uncalcined membrane layers (which refers to the solely prepared top layer, i.e., without any intermediate layer or support) were formed by pouring the sol into petri dishes and drying at the room temperature. Thermo gravimetric analysis (TGA, Perkin Elmer Diamond) was performed with dried powder for thermal characterization via a heating rate of 10 °C / minute. The dried powders were calcined at different temperatures, specifically at 400°, 500°, and 600 °C. The heating rate was 3 °C/minute and the samples were kept at target temperature for 150 min. X-ray diffraction (XRD, Philips Expert Pro) was used to determine the crystal structure of the unsupported membranes. A small amount of calcined powders was

dispersed in potassium chloride solution (10^{-3} M KCl) with varying initial pH and zeta potential measurements were performed by using a laser light–scattering electrophoresis measurement instrument (Zetasizer 3000HSA, Malvern, Co., UK).

Results and discussion

Sol preparation and characterization

Stable polymeric titania/zirconia sols either in sole or mixed form were prepared. Their particle size distributions were determined when fresh and after a year-long storage at refrigerator (4 °C). The average particle sizes (APS) were a few nanometers (< 6 nm), and sols were stable after a year-long storage as can be seen in Fig. 3. The error bars are indicating the deviation for consecutive measurements (at least five measurements) for the similar sol was very small. Consolidation, drying, and appropriate heat treatment of sols with such fine average particle size and size distribution values form a top layer with fine microporous structure [1, 2, 6, 13].

Thermal characterization of mixed Ti/Zr unsupported membranes

The calcination temperature determines the final morphological and physicochemical properties of the top layer of the ceramic composite membrane. Therefore, the thermal characterization of unsupported membranes is an important issue for preparation of ceramic membranes. The sols were dried, grounded, and thermally characterized via TGA (thermo gravimetric analysis) for monitoring the changes during the heat application. The TGA results for different recipes are shown in Fig. 4. There is a weight loss region due to the loss of free solvents (water and/or alcohol) at lower temperatures ($T < 200$ °C), followed by removal of bound solvents and organic residues (NO_x groups) at elevated temperatures. For Zr rich recipes, there is a distinct weight-loss region above 400 °C which may be related to crystallization.

Titania reached the gravimetric stability at around 350 °C losing ~ 30% of its weight while zirconia reached stability at around 480 °C losing 45% of its weight, as seen in Fig. 4. The thermogravimetric stability was achieved at higher temperatures for mixed oxides: 550 °C, 640 °C, and 580 °C for TiZr 7525, TiZr 5050, and TiZr 2575, respectively. The weight losses were 43%, 53%, and 43% for TiZr 7525, TiZr 5050, and TiZr 2575, respectively.

The profile for full Zr had three steps of weight loss: room temperature–250 °C, 250°–400 °C, 400°–480 °C. For Zr rich mixed oxides, the profile was somehow similar with the delaying of the weight loss for elevated temperatures. The boundary values for the weight loss steps in the TGA profiles changed from 400° to 480 °C and from 400° to 580 °C for TiZr7525 and TiZr5050, respectively, compared with full Zr.

The TGA profiles of Ti-rich recipes were relatively smoother. The first step can be considered from room temperature to ~ 200 °C and second from 200° to 340 °C. The boundary values for these steps were slightly different for varying Zr content. An additional distinct weight loss step was observed for TiZr2575 at elevated temperatures (from 520° to 640 °C) with the increasing Zr content.

Two possible reasons can be suggested for the shift in the TGA curves of ZrTi-mixed oxides. First one is the presence of interstitial carbon atoms in TiO2 or ZrO2 lattice which originate from the use of organic Ti or Zr precursors and organic solvents. Yurtsever and Çiftçioğlu [12] claimed that rare earth element doping caused a significant decrease in the pore size of TiO2. In this work, pore sizes in ZrTi mixed oxides may be lower than that of full Ti or full Zr. The possible presence of relatively narrower pores in ZrTi mixed oxides may delay the removal of residual carbonaceous species to higher temperatures than that of full Ti or full Zr. The TGA data in the considered temperature range (400° to 600 °C) (Fig. 4) is supporting the idea since the gravitational loss is postponed to elevated temperatures for mixed oxides. The second reason

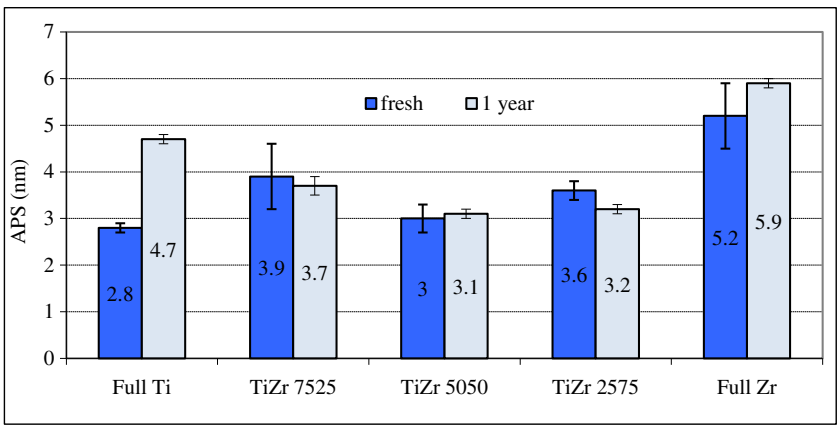

Fig. 3 The average particle sizes (APS) of fresh sols and after a year-long storage (error bars indicating the deviation of consecutive measurements of APS)

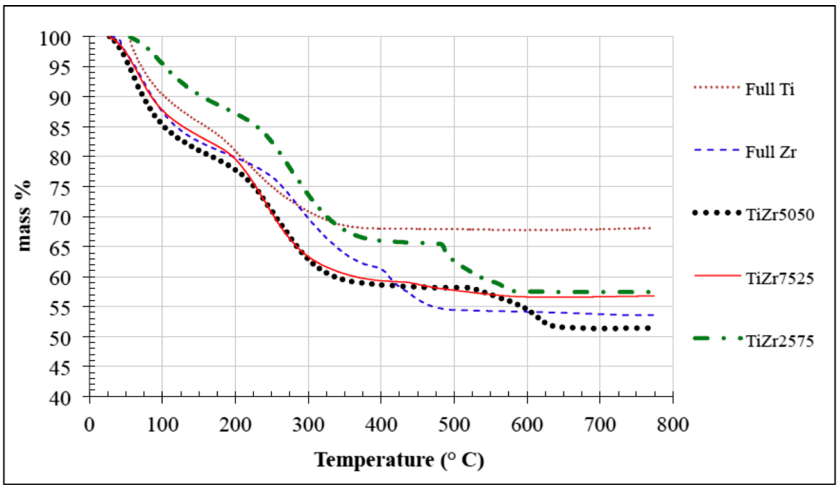

Fig. 4 TGA results for Ti/Zr unsupported membranes

may be the interstitial Zr atoms in the TiO2 lattice or interstitial Ti atoms in ZrO2 lattice. The mixing of Ti and Zr atoms in the atomic level may cause the formation of mixed oxide species $ZrTiO_4$ (or $Zr_xTi_yO_z$) as interactants through the sintering/phase transformation processes and formation of these compounds may be delayed by the presence of this interstitial accommodation. Differential calorimetric measurements in the study of Perez-Hernandez et al. [14] showed that exothermic peaks shifted towards higher temperatures in ZrTi oxides compared with that of single oxides indicating phase transformation retardation. It was also reported that they did not observe any segregation of $Zr_xTi_yO_z$ phases indicating high solubility of Ti and Zr in the host oxide. No other phases than TiO_2 or ZrO_2 were also detected in the XRD patterns of ZrTi mixed oxides in the reported work.

Crystallographic characterization of unsupported Ti/Zr membranes

The dried, ground Ti/Zr powders were heat treated at varying temperatures: 400°, 500°, and 600 °C for 150 min to prepare unsupported membranes. The crystal morphologies of these pure or mixed oxides were determined via XRD (X-ray diffraction, Philips X'PERT PRO) analysis. The samples were all amorphous before heat treatments.

Full Ti was composed only of anatase phase at 400 °C while the rutile phase occurred at 500 °C and increased at 600 °C as seen in Fig. 5, which is in agreement with the data reported by Zhang et al. [3]. TiZr 7525 was amorphous after heat treatment at 400 °C. The anatase phase formation initiation was observed at 500 °C, and it was well determined at 600 °C (Fig. 6). The first formation of the anatase phase for Ti-rich–mixed oxides was similarly reported before [6].

For TiZr5050, the first crystal peaks were determined at 600 °C for anatase and rutile titania and tetragonal and monoclinic zirconia as seen in Fig. 7, indicating the retardation of crystal formation to elevated temperatures.

TiZr 2575 was also amorphous after heat treatment at 400 °C (Fig. 8) like other mixed oxides. Anatase and rutile titania and tetragonal zirconia were determined at 500 °C, and their peak intensities increased at 600 °C.

Full Zr heat treated at 400 °C was in the tetragonal phase, as seen in Fig. 9. Van Gestel et al. [1] also reported the formation of tetragonal phase after calcination at 400 °C for 2 h. Aust et al. [6], in contrast, reported the crystallization of zirconia as the tetragonal phase at only after 500 °C, which may be due to shorter calcination time (1 h). Monoclinic phase occurred at 500 °C and increased at 600 °C, while its intensity was still low compared with the tetragonal phase. The formation of monoclinic phase in pure zirconia was also reported by Van Gestel et al. [1] at 450 °C but not mentioned by Aust et al. [6] or Benfer et al. [15].

The crystallite sizes of the calcined mixed and pure oxides were determined via the software of the XRD instrument (expert plus Scherrer calculator). The crystallites of pure titania (full Ti) was found more prone to the calcination temperature than the pure zirconia (full Zr) as shown in Fig. 10. The crystallite size values for full Ti increased from 12 to 42 nm, while the change was from 23 to 34 nm for full Zr, with the increasing calcination temperature. The crystallization of the mixed oxides started at higher temperatures. At 400 °C, all mixed oxides were in the amorphous phase. The greater susceptibility of titania to crystal growth with increasing calcination temperature was also observed for Ti-rich TiZr 7525, for which the crystallite sizes were the greatest in all samples. Interestingly, an increase in crystallite sizes was not observed for mixed oxides with increasing calcination temperature. The calcination duration (150 min) maybe was not sufficient for such observations. The crystallite sizes of mixed oxides calcined at 600 °C were comparable or smaller than the mixed oxides calcined at 500 °C. In the considered temperature range the Zr-rich oxides (Pure Zr, TiZr 2575, and even TiZr 5050) resulted in relatively smaller crystallite sizes at elevated calcination temperatures.

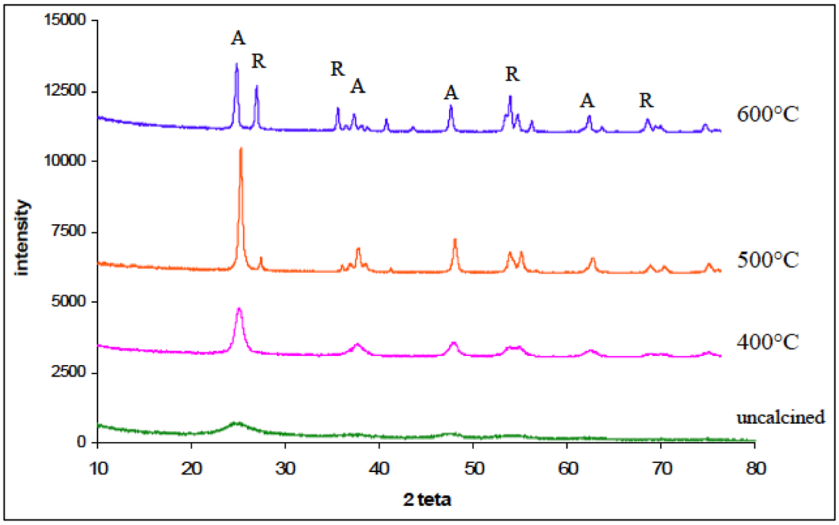

Fig. 5 XRD analysis spectrum for full Ti calcined at varying temperatures (A, anatase; R, rutile)

Crack/defect formation upon the heat treatment of ceramic bodies are known to be strongly related to their shrinkage behavior. Low percentage shrinkage values may contribute to the preparation of crack-free ultrafiltration/nanofiltration (UF/NF) membranes. The temperature range investigated in this work coincides with the heat treatment temperatures of the UF/NF membranes where the formation of cracks and pinholes may become possible. The XRD characterization results presented above indicated that the amorphous/crystalline phase transformations and most likely the nature of the packing/pore structure and surface properties of the nanostructure of these unsupported membranes can be controlled through the variation of the levels of zirconia doping of the titania-based membranes. The ionic sizes of Zr^{4+} and Ti^{4+} (68 and 72 pm ionic radii respectively) are very similar which can make substitutional doping relatively easy in composite Ti/Zr oxide structures [14]. The retarded phase transformations (nucleation and growth of anatase and rutile TiO_2, tetragonal, and monoclinic ZrO_2 phases) due to lower solid state diffusion in the substitutional solution creates a more defective structure along with controlled pore sizes in the 400–600 °C range used in this work. This may also increase the concentration of oxygen vacancies in the nanostructure which may generate enhanced catalytic properties and surface charges.

The first event of the nanostructure evolution occurs at around 100 °C and is most likely related to the densification due to packing/reorganization of polymeric species during the ethanol/water removal from the unsupported membrane pellet. This packing is likely to lead a small amount of volumetric shrinkage in the body. The second series of events observed between 200 and 400 °C may also be about the ongoing amorphous to crystalline transformation. Zirconium doping prevented the anatase to the rutile phase transformation. The main phase evolution event was observed in the 375–600 °C

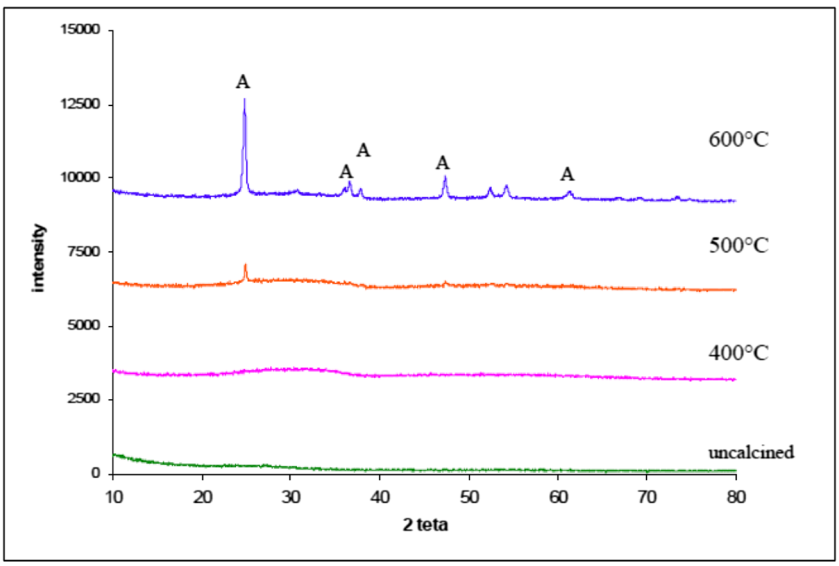

Fig. 6 XRD analysis spectrum for TiZr 7525 calcined at varying temperatures (A, anatase)

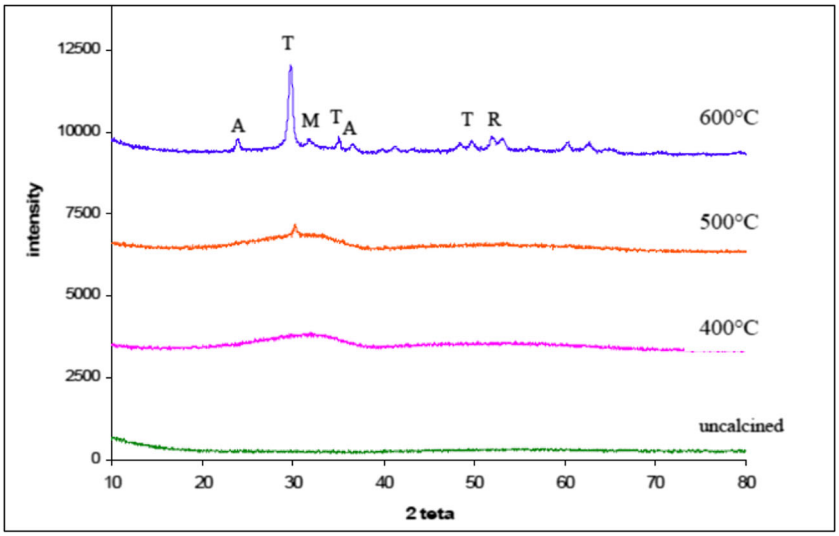

Fig. 7 XRD analysis spectrum for TiZr 5050 calcined at varying temperatures (A, anatase; M, monoclinic; R, rutile; T, tetragonal)

range for all powders which may be associated with anatase/rutile/tetragonal–monoclinic phase nucleation/crystallite growth/sintering/densification. The composition fundamentally determined the heat treatment temperatures of all of these phase evolution events. The TGA analysis indicated the presence of certain weight losses during these events as discussed earlier caused by the rearrangement of the well-packed precursor polymeric species.

Zeta potential (surface charge) of unsupported Ti/Zr membranes

The surface charges of the mixed or pure oxides heat-treated at different temperatures were determined via electrophoretic mobility measurements (Zetasizer 3000HSA, Malvern Co.). These measurements were performed by dispersing the oxides in potassium chloride solutions (10^{-3} M KCl) with initial pH values of 3.5, 7.2, and 9.8 to monitor the zeta potential values of the oxides in acidic, neutral, and basic media, respectively.

Acidic pH

Calcination at 400 °C At acidic pH, pure zirconia and titania, after calcination at 400 °C, possessed considerable positive surface charge while slightly positive zeta potential values were observed for mixed oxides (Fig. 11). The pure oxides (full Ti and full Zr), having a considerable positive surface charge at acidic pH, were in crystalline form while mixed oxides with low surface charge values were amorphous after calcination at 400 °C.

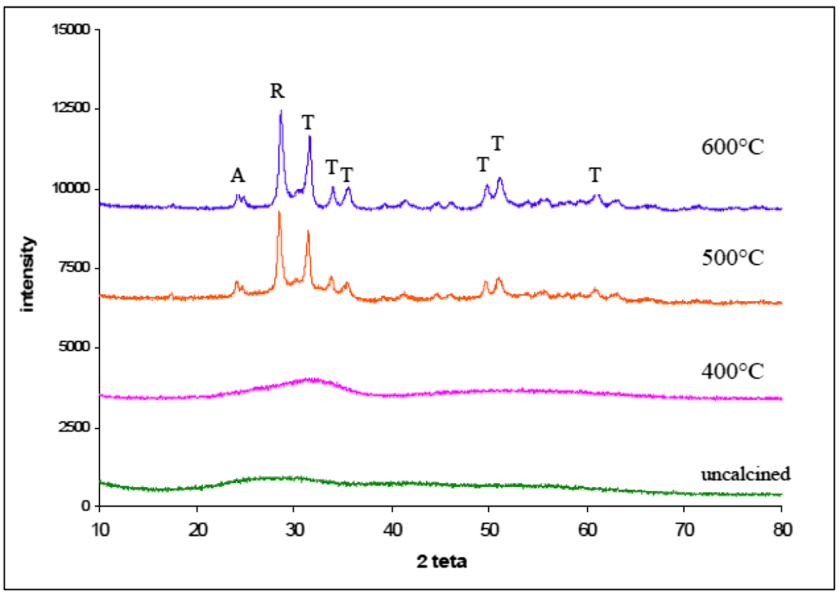

Fig. 8 XRD analysis spectrum for TiZr 2575 calcined at varying temperatures (A, anatase; R, rutile; T, tetragonal)

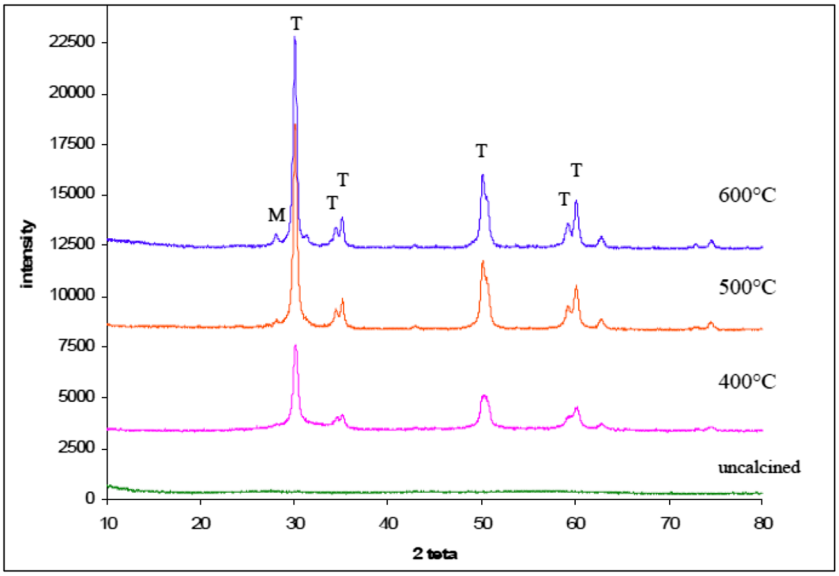

Fig. 9 XRD analysis spectrum for full Zr calcined at varying temperatures (M, monoclinic; T, tetragonal)

Calcination at 500 °C The zeta potential values for Zr-rich mixed oxides (TiZr 7525 and also TiZr 5050) increased by increasing calcination temperature (Fig. 11.). After calcination at 500 °C, zirconia-rich TiZr 2575 possessed the highest zeta potential value in which rutile, anatase, and the tetragonal phases were determined (Fig. 8.). For TiZr 5050, the initiation of formation of the tetragonal phase was determined after calcination at 500 °C. The zeta potential for full Zr decreased somehow with increasing calcination temperature, but still, it has a considerable positive value (22.9 mV).

Zeta potential values of titania-rich oxides were lower after calcination at 500 °C when compared to the values determined at 400 °C. The decrease was slight for the TiZr 7525 for which crystallization just initiates at that temperature. But for the pure titania (full Ti), the decrease was considerable. The XRD results show the phase transformation from anatase to rutile has occurred in full Ti at 500 °C up to some extent. That phase transformation may be effective on the considerable decrease of the positive surface charge. The analysis showed that the isoelectric point decreases after the anatase to rutile phase transformation (Fig. 12), showing the effectiveness of the phases on the surface charge properties. The initiation of the rutile phase formation was observed for full Ti at 500 °C while the anatase phase was still dominant. The anatase phase initiation was observed for TiZr7525 which was amorphous at 400 °C.

Calcination at 600 °C At 600 °C, the zeta potential values for zirconia-rich oxides were positive and high, while titania-rich oxides had slightly positive zeta potential, which may be again due to the anatase to rutile phase transformation, which even proceeded more for full Ti (Fig. 5). The zeta potential value for TiZr 7525 did not change considerably with the increasing temperature either, although the anatase phase formation was observed for the mixed oxide after calcination at 600 °C which was only initiated after calcination at 500 °C (Fig. 6).

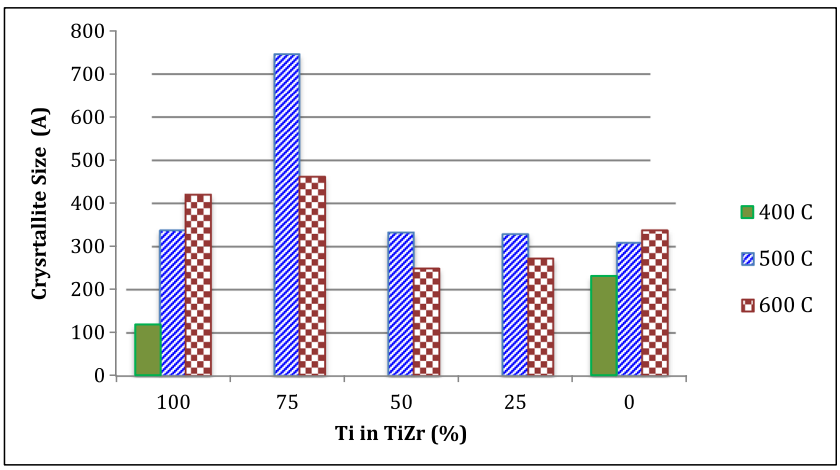

Fig. 10 The crystallite sizes (in angstroms) at different calcination temperatures

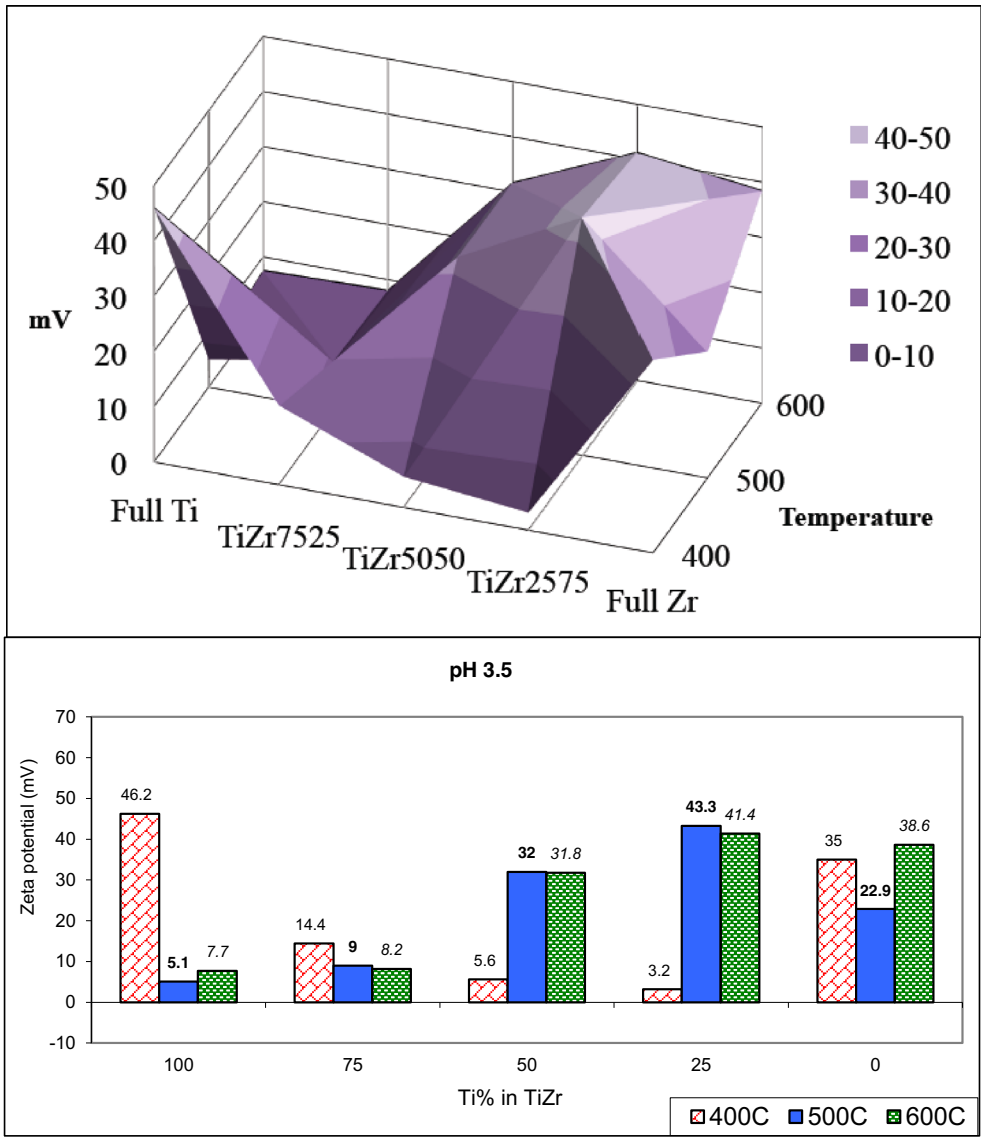

Fig. 11 Zeta potential values determined at acidic pH (3.5) in 10^{-3} M KCl solution

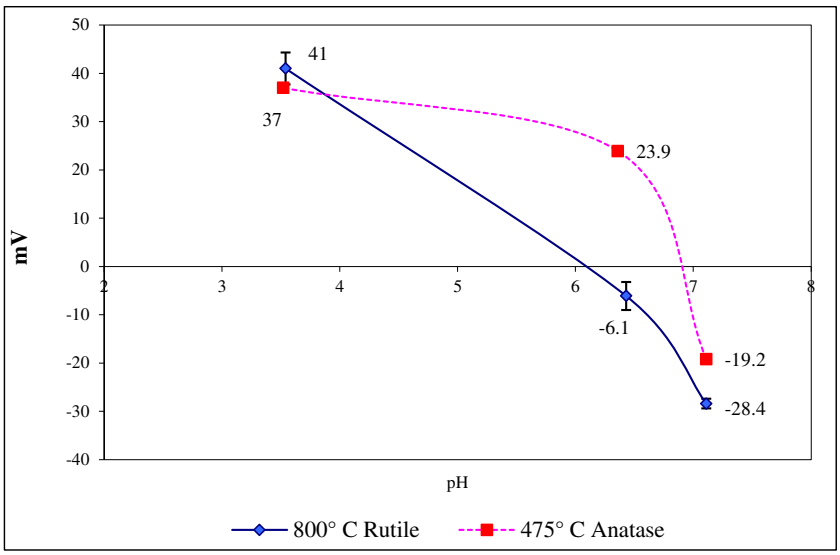

Fig. 12 Zeta potential values determined for pure anatase and rutile (titania) produced after calcination at different temperatures at various pH values

Neutral pH

At neutral pH, all oxide materials were almost neutral or negatively charged. Full Zr calcined at 600 °C possessed the highest negative zeta potential (Fig. 13). Its zeta potential was found to increase in magnitude with increasing calcination temperature, while it is not the case for full Ti. The magnitude of zeta potential of full Ti and TiZr 5050 decreased (to almost neutrality) with increasing calcination temperature (i.e., increasing crystallinity (Fig. 5 and Fig. 7)). Comparing TiZr 2575 and TiZr 7525, the zirconia-rich oxide possessed negative zeta potential higher in magnitude at varying calcination temperatures. The Zr-rich oxides (TiZr 25 75 and full Zr) gained higher negative surface charges with increasing calcination temperature (i.e., increasing crystallinity (Figs. 8 and 9)) at neutral pH values.

Basic pH

At basic pH, all oxides were negatively charged, as seen in Fig. 14. The magnitude of negative zeta potential values decreased considerably for titania-rich full Ti and TiZr 7525 with increasing calcination temperature. The decrease in the negative surface charge is considerable for full Ti calcined at 600 °C, where the anatase to rutile phase transformation was considerable (Fig. 5). For TiZr 7525, a very slight increase in negative surface charge was observed at 500 °C, where crystallization initiated and with the progress in crystallization the

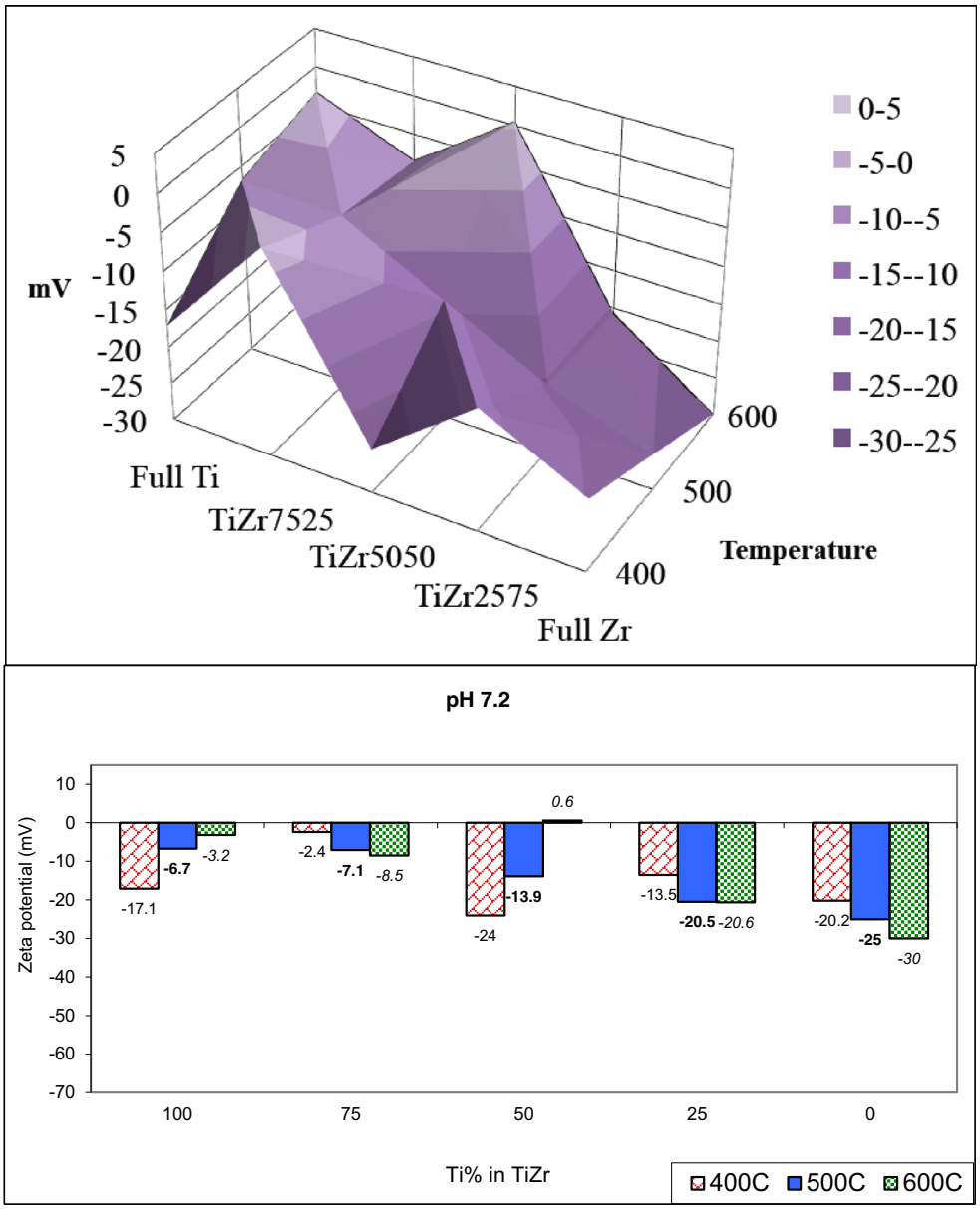

Fig. 13 Zeta potential values determined at neutral pH (7.2) in 10^{-3} M KCl solution

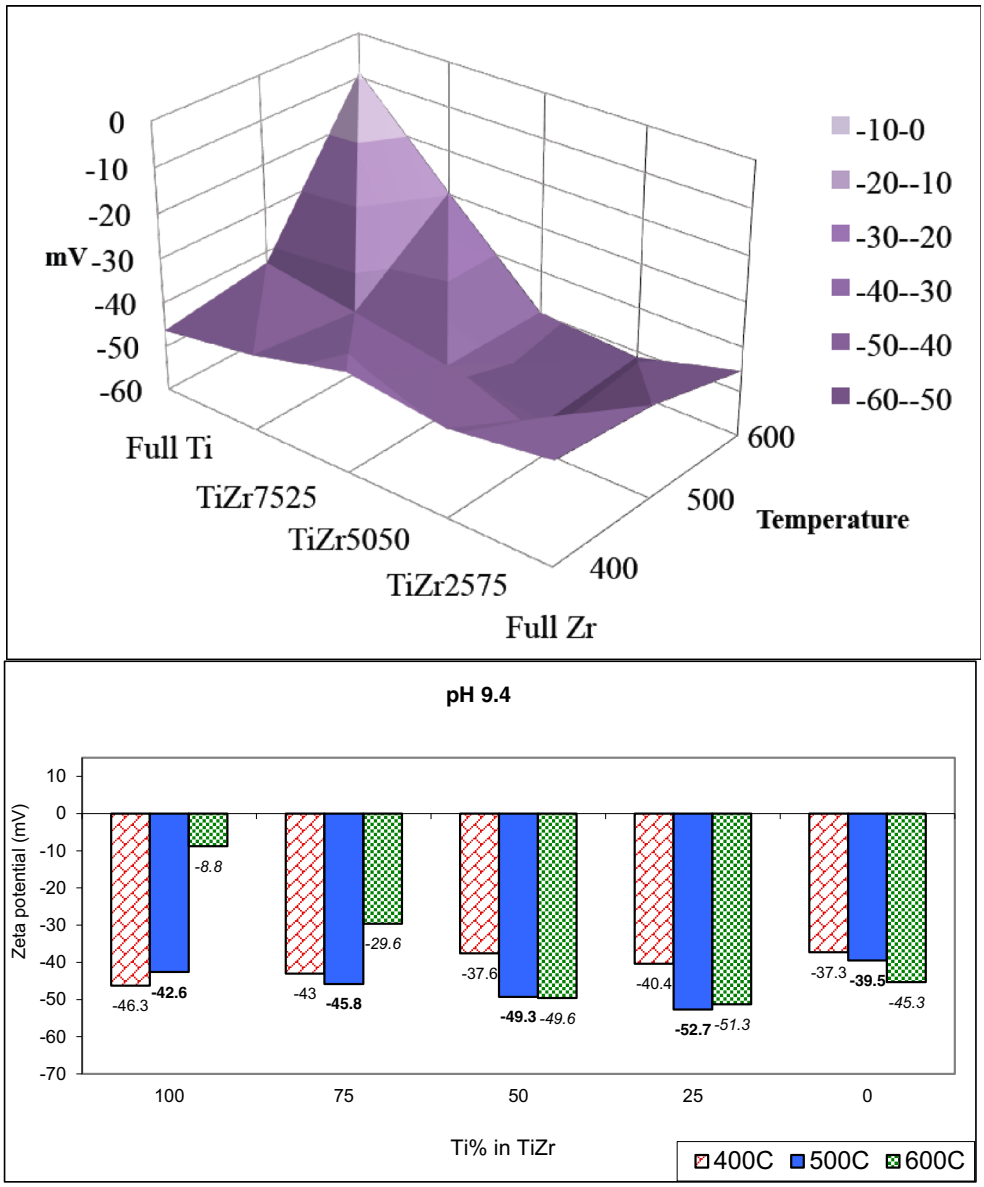

Fig. 14 Zeta potential values determined at basic pH (9.8) in 10^{-3} M KCl solution

magnitude of zeta potential decreased. The highest negative zeta potential value was possessed by Zr-rich TiZr 2575 calcined at 500 °C. For this sample, the negative surface charge values were higher at 500 °C and 600 °C calcination where there were considerable crystallization (Fig. 8). Similar trend was observed for TiZr 5050 where negative surface charge values were higher at 500 °C and 600 °C calcined samples for which crystallization has already initiated or in progress (Fig. 7). The zeta potential of full Zr slightly increased in magnitude by increasing calcination temperature (i.e., progressive crystallization (Fig. 9)).

The polymorphic titania/zirconia unsupported membranes possess different surface characteristics as discussed above. TiZr 2575 after calcination at 500 °C or above was composed of anatase and rutile titania and tetragonal zirconia. This structure gained the highest zeta potential values in magnitude at acidic and basic pH values. Increasing calcination temperature resulted in a decrease in the magnitudes of zeta potential for pure titania (full Ti) with the anatase to rutile transformation.

The removal of organic/ionic species from solutions by using membrane based UF/NF processes would have a great potential impact on energy efficient separation problems and environmental problems of today and the future. These ceramic nanostructures are preferred due to their superior chemical/thermal/mechanical properties compared with their polymeric counterparts which makes their utilization at relatively harsher conditions. The abilities developed on the nanodesign of these ceramic nanostructures may have a critical role on human living standards. The effect of zirconium mixing/other elemental doping on nanostructural evolution of the selective titania UF/NF membrane layers for the rejection of subnano-sized organic compounds/charged species should be further

investigated which may have significant implications in various applications.

The average particle size of the polymeric NF sol species/particles synthesized by sol-gel-based methods were determined to be in the 2–6 nm size range. The sol-species/particle-size distribution control through sol-gel chemistry and aging may constitute a fundamental issue in nanostructure development and subnano UF/NF membrane design. The oxide-doped UF/NF layers may experience lower levels of volumetric shrinkage of the body, retardations in phase structure evolution and decrease in crystallite size while they gain thermal stability which may contribute to obtaining crack-free selective membrane layers. Amorphous structures observed in titania-rich TiO_2-ZrO_2 mixed-oxide membranes may significantly contribute to the control/design of the micropore structure during the preparation of UF/NF membrane selective layers. The surface properties may also be controlled through processing and tuned towards specific separation problems.

The effect of Donnan exclusion mechanism is more important for the filtration/separation of charged materials with relatively smaller molecular weight. Therefore, the surface charge of the membrane top layer is a critical parameter for the separation efficiency during filtration applications in liquid media. The formation of tailor-made top layers with controlled surface characteristics was reported to be possible with the data presented. The sol-gel method used in the preparation of oxide layers enables preparation of mixed oxides starting from nano-sized clusters which are homogeneous in molecular level. The co-utilization of Zr and Ti with different electronegativities for preparation-mixed oxides via sol-gel method presented different opportunities. That difference in electronegativities of Zr and Ti and versatile probability of forming $Zr_xTi_yO_z$ with changing heat-treatment parameters during partial sintering resulted in versatile structures with necessary micro-porosity but also with varying types and quantities of defects in the microstructure (e.g., oxygen-deficient sites). These differences in the distribution of defects for (pure or mixed) oxides heat treated at different temperatures lead them to have varying surface characteristics (i.e., surface charge). This versatility of surface characteristics may also be important for different applications (e.g., catalysis), since oxides are being used as catalysts and/or catalyst supports [16].

Conclusion

The top layer of the ceramic composite membranes facing the fluid to be filtered is mainly responsible for the separation efficiency of the membranes. Its microstructure and physicochemical properties are important for both size exclusion and Donnan exclusion mechanisms. The formation of such a layer is possible by coating, drying, and calcination of nanoparticles prepared by using sol-gel method [12]. Stable Ti/Zr sols with a few nanometer average particle size were prepared with narrow particle-size distributions, which may be used for formation of top layers with fine microstructures.

The surface characteristics of the top layer can be altered by changing the titania/zirconia ratio and calcination temperature. The experiments performed by using unsupported Ti/Zr membranes showed the crystallization temperature increases when Ti and Zr are in mixed form. The magnitudes of zeta potential of the pure titania (full Ti) decreased with increasing calcination temperature. The Zr-rich unsupported membrane (TiZr 2575) possessed the highest zeta potential values at acidic and basic pH values after calcination at ≥ 500 °C. This polymorphic mixed oxide (TiZr 2575) was composed of anatase, rutile (titania), and tetragonal (zirconia) phases after calcination.

The results indicate the tailor-made top layers for ceramic composite membranes can be prepared by choosing appropriate Ti/Zr ratio and calcination conditions to have different surface characteristics to optimize the exclusion efficiency and decrease the fouling tendency. The results also may be helpful for ceramic membrane selection and/or predicting the possible separation efficiencies of current ceramic membranes for particular applications.

References

1. Van Gestel, T., Kruidhof, H., Blank, D.H.A., Bouwmeester, H.J.M.: ZrO2 and TiO2 membranes for nanofiltration and pervaporation. Part 1. preparation and characterization of a corrosion-resistant ZrO2 nanofiltration membrane with a MWCO < 300. J. Membr. Sci. **284**(1–2), 128–136 (2006)
2. Van Gestel, T., Sebold, D., Kruidhof, H., Bouwmeester, H.J.M.: ZrO2 and TiO2 membranes for nanofiltration and pervaporation. Part 2. development of ZrO2 and TiO2 toplayers for pervaporation. J. Membr. Sci. **318**(1–2), 413–421 (2008)
3. Zhang, H., Quan, X., Chen, S., Zhao, H., Zhao, Y., Li, W.: Zirconia and titania composite membranes for liquid phase separation: preparation and characterization. Desalination. **190**(1–3), 172–180 (2006)
4. Erdem, İ.: Sol-gel applications of ceramic membrane preparation. AIP Conf Proc. **1809**, 020011 (2017)
5. Van Gestel, T., Sebold, D., Hauler, F., Meulenberg, W.A., Buchkremer, H.: Potentialities of microporous membranes for H2/CO2 separation in future fossil fuel power plants: evaluation of SiO2, ZrO2, Y2O3-ZrO2 and TiO2-ZrO2 sol-gel membranes. J. Membr. Sci. **359**(1–2), 64–79 (2010)
6. Aust, U., Benfer, S., Dietze, M., Rost, A., Tomandl, G.: Development of microporous ceramic membranes in the system TiO2/ZrO2. J. Membr. Sci. **281**(1–2), 463–471 (2006)
7. Erdem, İ., Çiftçioğlu, M.: Influence of calcination temperature on microstructure and surface charge of membrane top layers composed of zirconia nanoparticles. J. Aust. Ceram. Soc. **51–1**(2015), 134–138 (2015)
8. Liang, L., Xu, Y., Hou, X., Wu, D., Sun, Y., Li, Z., Wu, Z.: Small-angle X-ray scattering study on the microstructure evolution of zirconia nanoparticles during calcination. J. Solid State Chem. **179**(4), 959–967 (2006)

9. Buchmeiser, M.: New synthetic ways for the preparation of high-performance liquid chromatography supports. J. Chromatogr. A. **918**(2), 233–266 (2001)
10. Almecija, M.C., Ibanez, R., Guadix, A., Guadix, E.M.: Effect of pH on the fractionation of whey proteins with a ceramic ultrafiltration membrane. J. Membr. Sci. **288**, 28–35 (2007)
11. Mazzoni, C., Orlandini, F., Bandini, S.: Role of electrolyte type on TiO_2-ZrO_2 nanofiltration membranes performances. Desalination. **240**, 227–235 (2009)
12. Erdem, İ., Çiftçioğlu, M., Harsa, Ş.: Preparation of ceramic composite membranes for protein separation. Key Eng. Mater. **264–268**(III), 2251–2254 (2004)
13. Shang, R., Verliefde, A.R.D., Hu, J., Zeng, Z., Lu, J., Kemperman, A.J.B., Deng, H., Nijmeijer, K., Heijman, S.G.J., Rietveld, L.C.: Tight ceramic UF membrane as RO pre-treatment: the role of electrostatic interactions on phosphate rejection. Water Res. **48**, 498–507 (2014)
14. Yurtsever, H.A., Çiftçioğlu, M.: The effect of rare earth element doping on the microstructural evolution of sol-gel titania powders. J. Alloys Compd. **695**, 1336–1353 (2017)
15. Benfer, S., Popp, U., Richter, H., Siewert, C., Tomandl, G.: Development and characterization of ceramic nanofiltration membranes. Sep. Purif. Technol. **22-23**, 231–237 (2001)
16. Perez-Hernandez, R., Mendoza-Anaya, D., Fernandez, M.E., Gomez-Cortes, A.: Synthesis of mixed ZrO_2-TiO_2 oxides by sol-gel: microstructural characterization and infrared spectroscopy studies of NO_x. J. Mol. Catal. A Chem. **281**, 200–206 (2008)